Carbohydrate Polymers 157 (2017) 114–121

Contents lists available at ScienceDirect

Carbohydrate Polymers

journal homepage: www.elsevier.com/locate/carbpol

Temperature stability of nanocellulose dispersions

Ellinor B. Heggset[a], Gary Chinga-Carrasco[a], Kristin Syverud[a,b,*]

[a] Paper and Fibre Research Institute (PFI), Høgskoleringen 6b, NO-7491 Trondheim, Norway
[b] Norwegian University of Science and Technology (NTNU), Department of Chemical Engineering, NO-7491 Trondheim, Norway

ARTICLE INFO

Article history:
Received 14 July 2016
Received in revised form 7 September 2016
Accepted 24 September 2016
Available online 25 September 2016

Chemical compounds studied in this article:
Sodium hypochlorite (PubChem CID: 23665760)
Sodium chlorite (PubChem CID: 23668197)
Sodium formate (PubChem CID: 2723810)
Cesium formate (PubChem CID: 23663999)
Furfural (PubChem CID: 7362)
Hydroxymethylfurfural (PubChem CID: 237332)

Keywords:
Cellulose nanofibrils
Cellulose nanocrystals
Rheology
Temperature stability
Drilling fluids
Enhanced oil recovery

ABSTRACT

Cellulose nanofibrils (CNF) have potential as rheology modifiers of water based fluids, *e.g.* drilling fluids for use in oil wells or as additives in injection water for enhanced oil recovery (EOR). The temperature in oil wells can be high (>100 °C), and the retention time long; days for drilling fluids and months for EOR fluids. Hence, it is important to assess the temperature stability over time of nanocellulose dispersions to clarify their suitability as rheology modifiers of water based fluids at such harsh conditions. Dispersions of CNF produced mechanically, by using TEMPO mediated oxidation and by using carboxymethylation as pretreatment, in addition to cellulose nanocrystals (CNC), have been subjected to heat aging. Temperature stability was best for CNC and for mechanically produced CNF that were stable after heating to 140 °C for three days. The effect of additives was evaluated; cesium formate and sodium formate increased the temperature stability of the dispersions, while there was no effect of using phosphate buffer.

1. Introduction

1.1. Nanocellulose

Wood-based nanocelluloses comprise two main groups, *i.e.* cellulose nanofibrils (CNF) and cellulose nanocrystals (CNC). Disintegration of cellulose fibers into CNF was first described by Turbak, Snyder, and Sandberg (1983) and Herrick, Casebier, Hamilton, and Sandberg (1983) using conventional homogenization of wood pulp. This method is often referred to as mechanical production. Since then, production methods combining chemical pretreatment with mechanical disintegration have been introduced, *e.g.* 2,2,6,6-tetramethylpiperidine-1-oxyl radical (TEMPO)-mediated oxidation (Saito, Nishiyama, Putaux, Vignon, & Isogai, 2006) and mild carboxymethylation (Wågberg et al., 2008). The resulting CNF materials vary in morphology and surface chemistry (Klemm et al., 2011). CNC is produced by hydrolyzing the amorphous parts of cellulose with mineral acids, followed by removal of the residual acids and impurities, and sonication for separation of the crystals (Brinchi, Cotana, Fortunati, & Kenny, 2013; Dong, Revol, & Gray, 1998; Habibi, Lucia, & Rojas, 2010; Lin, Huang, & Dufresne, 2012; Rånby, 1951).

The viscosifying properties of CNF were mentioned in the first patents in the beginning of the 1980's (Turbak, Snyder, & Sandberg, 1982, 1985). Applications in food, emulsions, cosmetics and in fluids for drilling operations have been suggested. Due to an energy intensive production process, the commercial interest was limited for several years. However, during the last years, breakthroughs in the production of nanocellulose have been achieved and the energy consumption has been reduced considerably (Henriksson, Henriksson, Berglund, & Lindstrom, 2007; Pääkkö et al., 2007). Thus, the interest in the material has been renewed.

* Corresponding author at: Paper and Fibre Research Institute AS (PFI), Høgskoleringen 6b, NO-7491 Trondheim, Trondheim, Norway. Tel.: +47 95 90 37 40.
E-mail addresses: ellinor.heggset@pfi.no (E.B. Heggset), gary.chinga.carrasco@pfi.no (G. Chinga-Carrasco), kristin.syverud@pfi.no (K. Syverud).

http://dx.doi.org/10.1016/j.carbpol.2016.09.077
0144-8617/

1.2. Drilling fluids/EOR

Rheology is important in several fluids used in the oilfield industry, *e.g.* in drilling fluids and in chemical flooding for enhanced oil recovery (EOR). Water based drilling fluids apply various components to modify the rheology, *e.g.* carboxymethyl cellulose (CMC), guar gum and xanthan gum (Caenn & Chillingar, 1996). At high temperature and high pressure conditions (HTHP), these organic rheology modifiers do not perform adequately, as their viscosity is reduced due to change in conformation or decomposition (Chang, 1978; Thomas, 2008). Additionally, the alternative synthetic polymers that are stable at high temperatures are associated with environmental concerns. The chemical additives used commercially in EOR are polyacrylamide or polyacrylamide derivatives (Abidin, Puspasari, & Nugroho, 2012; Zhu, Wei, Wang, & Feng, 2014). However, due to environmental concerns associated with these chemicals, the use is prohibited by many countries (Force, 2011).

1.3. Temperature stability

Temperature stability is an important criterion for both drilling fluids and in EOR. According to a study of Chen, Zhu, Baez, Kitin, and Elder, (2016), native cellulose decomposes at around 275 °C while CNC (produced using conventional concentrated sulfuric acid hydrolysis) had a degradation temperature around 220 °C. The experiment was done in dry state and with nitrogen atmosphere (Chen et al., 2016) In another study, degradation temperature of fibrils produced by TEMPO-mediated oxidation was compared to degradation temperature of native cellulose, also using nitrogen atmosphere. The decomposition temperature was significantly lower for the TEMPO oxidized cellulose 220 °C compared to 275 °C for native cellulose (Fukuzumi, Saito, Okita, & Isogai, 2010). In TEMPO-oxidized material, the fibrillation process itself has been found to affect the thermal degradation temperature minimally (Johnson, Zink-Sharp, Renneckar, & Glasser, 2009).

In industrial applications like drilling fluids or for EOR, both water, oxygen and several ions are present. Therefore, thermogravimetric analyses (TGA) that are performed in dry state and atmosphere without oxygen has limited relevance as other degradation temperatures are expected under the relevant conditions. Carbohydrate polymers like xanthan and carboxymethylcellulose are used in drilling fluids and are suggested as additives in EOR. However, in oil reservoirs acid, alkali and redox reactions can potentially degrade polysaccharides. Acid hydrolysis in which the glycosidic bond in polysaccharides is cleaved under uptake of a water molecule is well documented. Reservoir pH is in the neutral range (pH 6–8), and acid hydrolysis is probably of minor importance for degradation. The glycosidic linkage cleaves slowly in alkali and requires temperatures above 150 °C (Kleppe, 1970; Rydholm, 1955). It is thus likely that radical, oxidative/reductive depolymerization (ORD) reactions are responsible for polymer degradation at normal reservoir conditions below 150 °C. Free radicals have one or more unpaired electrons that can attack polymers. Biopolymers are susceptible for autoxidation, *i.e.* direct reaction with O_2 forming radicals which readily react with O_2 producing a hydroperoxide radical. This leads to propagating chain reactions. Several different reaction paths for hydroperoxide decomposition are possible. Transition metals and heat increase the decomposition (Wellington, 1983). All carbohydrate polymers are susceptible to such decomposition mechanisms. Our hypothesis is that nanocelluloses are less vulnerable in this respect due to their structure in which the cellulose polymer chains are organized in bundles with high degree of crystallinity.

In the present work we assessed the thermal stability of various qualities of nanocellulose. The tested samples include mechanically produced CNF, carboxymethylated CNF, TEMPO oxidized CNF and CNC. For comparison, samples of xanthan and guar gum were also included in the study. It has been shown that salts of formic acid raise temperature stability of xanthan by acting as a free-radical scavenger. Hence, the effect of using cesium and sodium formate as additives on the thermal stability of nanocellulose dispersions has been assessed. In addition, buffer at neutral pH was added to some samples to shed light of the effect of acid hydrolysis.

2. Experimental section

2.1. Chemicals

The cellulose nanocrystals (CNC) used in this study were purchased from the University of Maine (see below). The cesium formate solution was kindly provided by Cabot Corporation (Howard, Kaminski, & Downs, 2015). All other chemicals were of laboratory grade quality purchased from Sigma Aldrich.

2.2. Nanocellulose production and characterization

Never-dried softwood bleached pulp fibres were used as the source material for production of three nanocellulose qualities. The first quality was produced using a mechanical pretreatment, *i.e.* beating in a Claflin mill (1000 kWh/ton for 1 h; Mech-CNF). Production of the second quality was performed using TEMPO mediated oxidation (TEMPO-CNF), as described by Saito and colleagues in 2006 (Saito et al., 2006). 2.2 mmol NaClO per gram cellulose was used in the oxidation. The third quality was produced using low substituted carboxymethylation as pre-treatment (Carboxy-CNF) (Wågberg et al., 2008). The fibrillation was done by using a Rannie 15 type 12.56× homogenizer (APV, SPX Flow Technology, Silkeborg, Denmark), with a pressure drop of 1000 bar in each pass. The mechanical quality was collected after 5 passes, the TEMPO oxidized quality after 1 pass and the carboxymethylated quality after 2 passes through the homogenizer. The consistency of all samples before homogenization was 1%.

The cellulose nanocrystals (CNC; 11.7 wt%) were procured from the University of Maine (Orono, USA). The material was manufactured at the US Forest Service's Cellulose Nano-Materials Pilot Plant at the Forest Products Laboratory (FPL; Madison, Wisconsin). The cellulose nanocrystals were produced using sulphuric acid (64%) to hydrolyze the amorphous regions of the cellulose material, producing acid resistant crystals (Dong et al., 1998).

The content of carboxyl and aldehyde groups was determined by conductometric titration, as described by Saito and Isogai (Saito & Isogai, 2004), using an automatic titrator (Metrohm 902 Titrando). The carboxylate content was calculated from the titration curve (Gran plot). This analysis was also done after oxidation of aldehyde groups to carboxyl groups with $NaClO_2$ in order to estimate the content of aldehyde groups. The degree of polymerization (DP) was estimated from intrinsic viscosity values determined according to the standard ISO 5351:2010. The intrinsic viscosity was assessed before the homogenization of the pre-treated pulp fibres. The DP was calculated using the following equation: $DP^{0.905} = 0.75\ [\eta]$, where $[\eta]$ is the intrinsic viscosity (Sihtola, Kyrklund, Laamanen, & Palenius, 1963).

SEM imaging was performed with a Hitachi scanning electron microscope (SEM, SU3500), in secondary electron imaging mode. AFM imaging was performed with a Multimode AFM (with Nanoscope V controller), Digital Instruments. All images were recorded in ScanAsyst mode (peak force tapping mode), at room temperature in air. The AFM tips of spring constant value ~0.4 N/m were purchased from Bruker AFM probes.

Table 1
Sample overview: nanocellulose dispersions and reference polymers.

Sample code	Nanocellulose quality/polymer	Additive
Mech-CNF	Mechanical CNF	None
Mech-CNF-Na	Mechanical CNF	Na-Formate[a]
Mech-CNF-Cs	Mechanical CNF	Cs-Formate[a]
Mech-CNF-P	Mechanical CNF	Phosphate buffer
CNC	CNC	None
CNC-Na	CNC	Na-Formate
CNC-Cs	CNC	Cs-Formate[a]
CNC-P	CNC	Phosphate buffer
TEMPO-CNF	TEMPO CNF	None
TEMPO-CNF-Na	TEMPO CNF	Na-Formate
Carboxy-CNF	Carboxymethylated CNF	None
Carboxy-CNF-Na	Carboxymethylated CNF	Na-Formate
Xanthan	Xanthan gum	None
Xanthan-Na	Xanthan gum	Na-Formate
Guar	Guar gum	None
Guar-Na	Guar gum	Na-Formate

[a] The additives were tested in two concentrations, 0.066 M and 0.37 M.

2.3. Temperature stability

In order to assess the temperature stability of the nanocellulose dispersions, they were heated to temperatures ranging from 110 to 150 °C in air atmosphere, and kept at the elevated temperature for 3 days. A solid content of 0.8 wt% was used in all experiments as this is a relevant concentration for drilling fluids. This corresponds to typical conditions used to test drilling fluids by the oil industry. A Parr Pressure Reactor was used for the heating, together with a Parr 4838 Reactor controller and a heating mantle. The samples were mixed in bottles of Teflon, and stirred vigorously. The bottles were sealed to avoid evaporation.The pressure reactor was preheated to 60 °C. The temperature in the reactor was measured using both an internal and an external gauge, and the reaction time was started when the internal temperature reached the required temperature.

The effect of various additives on the temperature stability of mechanically produced CNF and CNC dispersions was tested and compared to dispersions without additives, *i.e.* nanocellulose dispersed in pure water. The additives were cesium formate, sodium formate and phosphate buffer (pH 7) with the following concentrations; 0.066 M, 0.066 M and 0.068 M, respectively. Addition of a higher concentration of cesium formate, 0.37 M, was also tested, to assess the effect of higher salt concentration. The phosphate buffer was prepared by mixing 1 M Na_2HPO_4 and 1 M NaH_2PO_4. The final concentrations of fibrils/crystals were 0.8% in all samples. This corresponds to a monosaccharide concentration of 0.05 M, meaning that the additives are in excess compared to the glucose monomers in all samples.

The temperature stability of the four nanocellulose qualities was compared without and with sodium formate as additive. The samples were heated to 130, 140 and 150 °C, and incubated in the reactor for three days at each temperature level. The same experiments were done for samples of xanthan and guar gum (0.8%) at 140 °C. The pH was assessed in all samples before and after the heating. The assessed samples and compositions are listed in Table 1.

2.4. Determination of color-change

Films of 10 g/m^2 were prepared by solvent casting of the nanocellulose dispersions, both before and after heating. The color of the films was assessed based on digitally scanned images. The images were acquired with an Epson Perfection scanner. The resolution was 2400 dpi, corresponding to a pixel size of 10.6 μm and the films (diameter = 14 mm) were scanned in reflection mode. The greylevel of each sample was quantified. A white background was used as backing during image acquisition. The greylevel of the films before heating (20 °C) was used as control within each series. The color-change was thus estimated according to the following Eq. (1):

$$\text{Color-change}: \left(1 - \frac{greylevel_i}{greylevel_c}\right) \times 100 \quad (1)$$

Where $greylevel_i$ corresponds to the greylevel of film i and $greylevel_c$ corresponds to the greylevel of the control film before heating within each series.

2.5. Determination of degradation products

To determine the degradation products after heat aging, ultraviolet – visible (UV–vis) spectroscopy was performed on nanocellulose dispersions with and without sodium formate as additive, before and after heat aging at 140 °C for three days. Samples were centrifuged to remove precipitates, and the supernatant was diluted and analyzed. A sweep for wavelengths from 200 to 800 nm was performed (results not shown) and a peak was detected at 277 nm. Furfural and hydroxymethylfurfural (HMF) are well known degradation products from pentoses and hexoses respectively (Dunlop, 1948), both with absorption at this wavelength. The samples were thus further analyzed at this wavelength to estimate the amounts of furfural/HMF (in mg/mL). A reference sample of sodium formate was also analyzed, and it was verified that it does not give an absorbance peak at 277 nm.

2.6. Rheological measurements

The rheological properties of nanocellulose dispersions were measured on a Physica MCR-301 (Anton Paar GmbH, Graz, Austria) rotational rheometer, using the RheoPlus software, as previously described (Iotti, Gregersen, Moe, & Lenes, 2011). The Physica MCR-301 was used in controlled shear mode to test the shear rate/time dependency of 0.8% dispersions of nanocellulose. The rheometer was equipped with a temperature controlled lower plate (P-PTD200/62/TG), and the temperature was maintained at 20 °C. A conical-plate geometry type was selected as the most appropriate for the measurements (McClements, 2004), and the conical geometry (CP40-2/s) was serrated to prevent wall slip. The gap between the geometries was 1 mm and the sample was allowed to rest 10 min before starting the measurements. Specific covers around samples and distilled water on the geometries were used to prevent sample drying during the experiments. The shear rates investigated for all measurements were between 0 and 1000 s^{-1}.

3. Results and discussion

3.1. Nanocellulose characteristics

AFM images of the nanocellulose samples are shown in Fig. 1. The mechanical CNF has coarser structure than the TEMPO oxidized and the carboxymethylated samples (Fig. 1A–C), as demonstrated previously by various authors (Chinga-Carrasco et al., 2012; Chinga-Carrasco, Yu, & Diserud, 2011; Saito et al., 2006; Wågberg et al., 2008). The morphology of CNC used in this study is exemplified in Fig. 1D, and also described in previous literature (Bras, Viet, Bruzzese, & Dufresne, 2011; Habibi et al., 2010). Some structural and chemical nanocellulose characteristics are summarized in Table 2.

3.2. Effect of additives

The effect of using the additives cesium formate and sodium formate was studied (Table 3). Dispersions of Mech-CNF and CNC without additive and with sodium formate and cesium formate

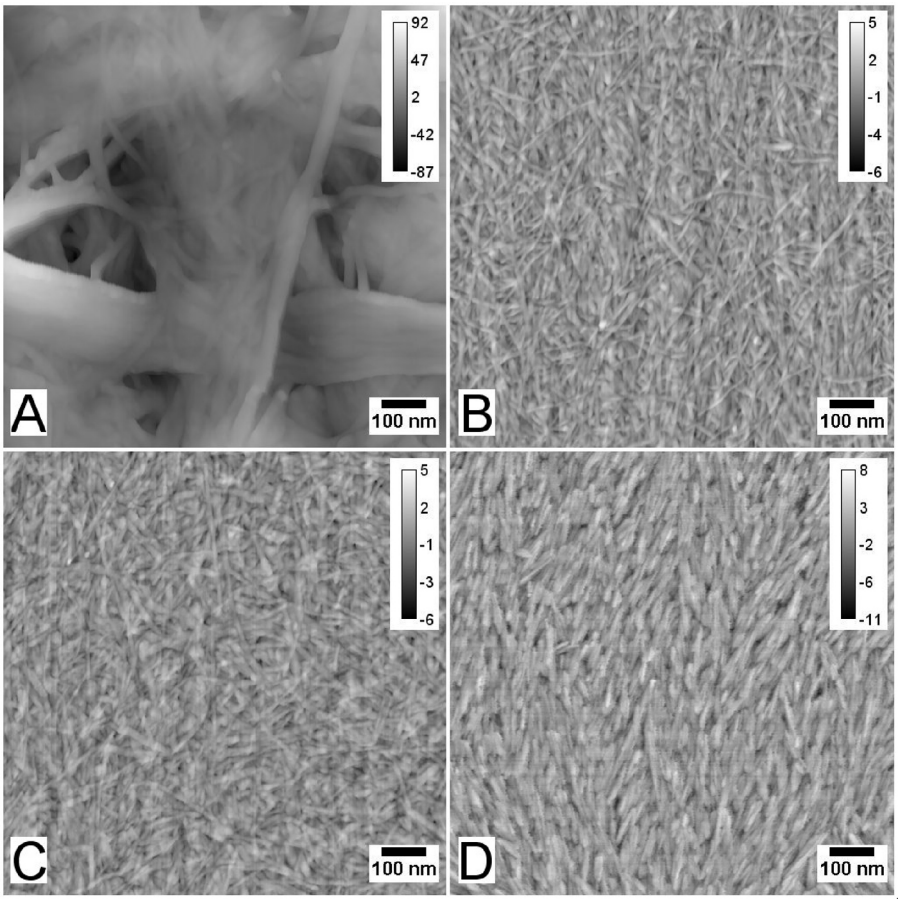

Fig. 1. AFM images of the nanocellulose samples; Mech-CNF (A), TEMPO-CNF (B), Carboxy-CNF (C) and CNC (D). The calibration and scale bars are in nanometers.

Table 2
Nanocellulose characteristics.

Sample	Charge density[a] (mmol/g)	Intrinsic viscosity (ml/g)/DP	Fibril diameter (nm)	Fibril length (μm)	Functional groups in significant amounts
Mech-CNF	0.1	620/890	<100	>1	−OH, −COOH
TEMPO-CNF	0.9[b]	450/620	<20	>1	−OH, −CHO, −COOH
Carboxy-CNF	0.4	–	<20	>1	−OH, $-CH_2COOH$
CNC	approx. 0.3[c]	80/90	<20	<0.2	−OH, $-SO_3H$

[a] This is carboxylic acids for Mech-CNF, TEMPO-CNF and Carboxy-CNF. For CNC the charged groups are sulphate half ester.
[b] Aldehyde content determined by conductometric titration; 0.2 mmol/g CNF.
[c] Determined by inductively coupled plasma – atomic absorption (ICP-AA).

Table 3
pH in nanocellulose dispersions before and after heat aging for 3 days at various temperatures. Change in pH and the number of H^+ formed per thousand monosaccharide glucose units after heat aging at 140 °C for three days. A variation of ± 5 °C in temperature was observed during the heat aging tests. For the pH measurements, a standard deviation was typically found to be 0.05 after five pH measurements, a value that was representative for all the dispersions.

Sample	Start pH	pH after 3 days				Δ pH, 3 days at 140 °C	H^+ formed in ‰ of glucose units (140 °C)
		110 °C	130 °C	140 °C	150 °C		
Mech-CNF	7.2	5.8	3.2	3.5	3.2	3.7	65
Mech-CNF-Na	7.6	6.4	6.3	5.6	5.4	2.0	0.5
Mech-CNF-Cs	10.2		6.8	6.6		3.5	0.1
CNC	7.2	2.8	2.7	2.7	2.7	4.5	400
CNC-Na	6.7	6.0	4.2	5.8	5.3	0.9	0.3
CNC-Cs	10.3			6.2		4.1	0.1

were subjected to heat treatment for three days at 110, 130, 140 and 150 °C.

Reduction of pH is an indication of degradation and is caused by inter- and intramolecular degradation reactions, which form different degradation products (described in the next sections). Larger pH-change indicates more degradation. Table 3 shows changes in pH for the Mech-CNF and CNC samples with and without the additives Na-formate and Cs-formate. All samples undergo a reduction in pH after heat aging, confirming the formation of acidic groups at all the tested temperatures. The samples with no additives have the largest pH-changes; 3.7 and 4.5 pH units for Mech-CNF and CNC, respectively.

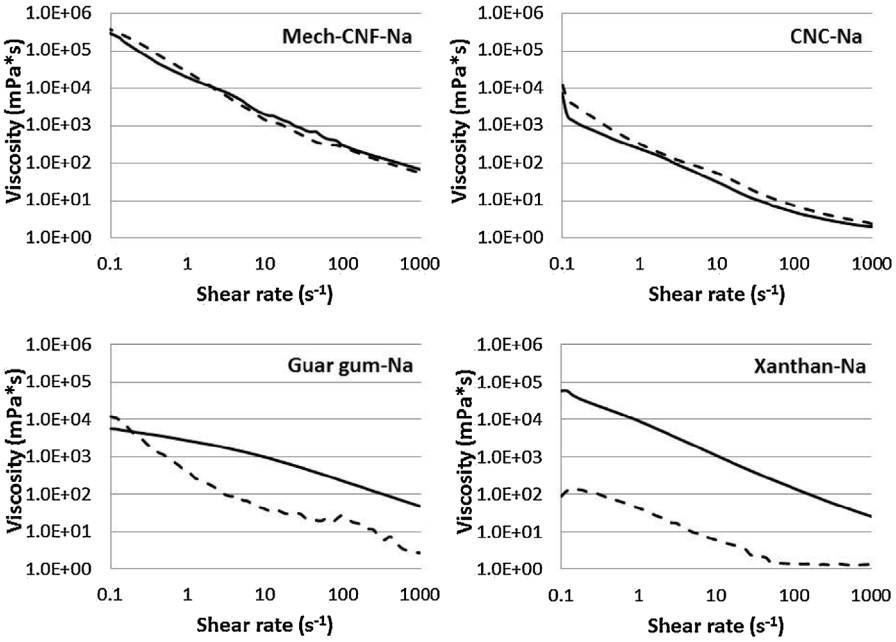

Fig. 2. Viscosity as a function of shear rate for nanocellulose dispersions, xanthan and guar gum with sodium formate added, before (solid line) and after heat aging at 140 °C (dotted line) for three days. All samples had a solid content of 0.8%.

As the start pH varied between the samples, the change in pH cannot be compared directly.

For adequately comparing the degradation of the samples, the number of H^+ units formed per thousand glucose units in the polymer chain during the heat aging at 140 °C was estimated from the pH-values (see Table 3). Both cesium formate and sodium formate lowered the number of H^+ formed per thousand glucose units significantly, by an order of 10 to 100. The decomposition of the samples without additives is substantial; 65 and 400H^+ per 1000 glucose units for Mech-CNF and CNC, respectively.

During thermo-oxidative degradation of cellulose, a number of reactions will lead to formation of C=O and C=C bonds. It is, for instance, suggested that elimination of water involving the ring hydroxyl groups will lead to formation of C=C bonds. In the case of CNC, desulfation will probably also occur. The released sulfuric acid molecules can further facilitate removal of ring hydroxyl groups by either direct catalysis of the removal of water or esterification of the hydroxyl groups with subsequent removal of sulfuric acid (Julien, Chornet, & Overend, 1993; Roman & Winter, 2004). This can be a possible explanation for the high amount of H^+ formed for the samples with CNC (Table 3), already after heat aging at 110 °C.

Phosphate buffer as additive was also tested in order to verify if neutralization of potentially formed acids could reduce the decomposition rate, compared to the samples with no pH stabilization. Compared to the formate-additives, negligible pH-changes were found in the samples with phosphate buffer, for both concentrations of buffer. This was as expected and indicates that the buffer capacity was sufficiently high. The buffer will stabilize pH by neutralization of acid groups that may be formed due to degradation. Assessment of degradation was thus done by measuring the viscosity profiles of these samples.

Reduction of viscosity is a sign of degradation and depolymerization. The effect of the additives on the viscosity of the samples is shown in Fig. S.1. in Supplementary material. Comparing CNF with and without buffer at 25 °C showed similar viscosity profile, confirming that there was no effect on viscosity by adding buffer itself. Comparison of a CNF dispersion in pure water, before and after heat aging, showed a lowering of the viscosity profile, indicating decomposition of the CNF. The same observation was done for samples in which phosphate buffer was added (Fig. S.1.A). The stabilization of pH did not prevent decomposition of cellulose. This indicates that acid hydrolysis is not the main decomposition mechanism. The samples containing cesium formate and sodium formate additives had smaller shifts in the rheology profile, compared to the samples without additives or by using phosphate buffer (Fig. S.1.B). The results indicate that oxidative-reductive depolymerization (ORD) is the main decomposition mechanism and that the formate ions, known to be an anti-oxidant that scavenges hydroxyl radicals, protect cellulose against this (Downs, 1992).

As described in Table 1, the addition of cesium formate was tested in two concentrations, 0.066 M and 0.37 M, respectively. The experiments showed that a change in concentration did not affect/reduce the viscosity (results not shown). Hence, for further experiments, a concentration of 0.066 M was used for the different additives.

3.3. Temperature stability of different nanocellulose qualities

The results from the trials that compared different additives (Table 3 and Fig. S.1.), showed that both cesium and sodium formate improved the temperature stability of nanocellulose. Sodium formate was used in further experiments. The temperature stability of four different nanocelluloses was thus assessed with and without sodium formate as additive. pH-values for the samples after heat aging are shown in Table 4. The samples had a start pH between 6.6 and 7.8. The pH-change after heat aging was systematically lower for the samples having sodium formate as additive, confirming the results from the previous section. The number of formed H^+ per thousand glucose units showed almost the same pattern for all the CNF samples; 20–65H^+/1000 glucose units without additive, and a reduction to roughly 1H^+/1000 glucose units with additive. For the CNC sample, the difference was larger, from 400H^+/1000 glucose units without additive to 0.3H3H^+/1000 glucose units with additive, as also described in the previous section.

The viscosity profiles of the Mech-CNF, CNC, xanthan and guar gum, before and after heat aging, are shown in Fig. 2. All samples were with sodium formate and no sign of coagulations was seen in

Table 4
pH in various nanocellulose dispersions before and after heat aging for three days at temperatures from 110 °C to 150 °C. Change in pH and H^+ formed per thousand glucose units after heat aging at 140 °C for three days. For the pH measurements, a standard deviation was typically found to be 0.05 after five pH measurements, a value that was representative for all the dispersions.

Sample	Start pH	pH after 3 days				Δ pH, 3 days at 140 °C	H^+ formed in ‰ of glucose units (140 °C)
		110 °C	130 °C	140 °C	150 °C		
Mech-CNF	7.2	5.8	3.2	3.5	3.2	4.0	65
Mech-CNF-Na	7.5	6.4	6.3	5.6	5.4	2.1	0.5
TEMPO-CNF	7.2	4.1	4.2	4.0	3.9	3.3	20
TEMPO-CNF-Na	6.8	5.3	5.1	5.2	4.9	1.9	1
Carboxy-CNF	7.2	3.9	–	3.6	3.6	3.6	50
Carboxy-CNF-Na	6.9	5.8	5.3	4.9	4.9	2.0	3
CNC	7.8	2.8	2.7	2.7	2.7	5.1	400
CNC-Na	6.6	6.0	5.8	5.8	5.3	1.3	0.3

the samples before heat aging. There were only small shifts in the viscosity profile for Mech-CNF and CNC.

Xanthan and guar gum had a large reduction in the viscosity profile after heat aging. The viscosity profiles of the various nanocellulose dispersions shift towards lower viscosity as cellulose/hemicellulose is broken down to low molecular components. However, increase in viscosity was also observed (see *e.g.* Fig. 2 for the CNC sample). We believe that this was caused by formation of acid groups on the cellulose backbone and molecules that were released from the solid cellulose fibril structure and transferred to the water phase as dissolved molecules. This may occur before a potential shortening of the cellulose chains arises. Such phenomena could initially increase viscosity. It is worth to mention that phase separation and formation of gelatinous lumps was observed in samples of TEMPO-CNF and Carboxy-CNF, indicating such changes.

3.4. Color-change

Changes in color from colorless/white to yellow/brownish/black are signs of carbohydrate decomposition, and such decomposition will occur during heat aging at certain temperature levels (Matsuo, Umemura, & Kawai, 2012; Yatagai & Zeronian, 1994). Thus color-change is an important parameter to assess when studying temperature stability of carbohydrates. Although the mechanism of the color-change has been discussed, it has not been fully clarified yet (Matsuo et al., 2012; Zervos & Moropoulou, 2005). Thermal oxidation, which occurs in the presence of oxygen, is suggested as a relevant reaction mechanism. Aldehyde and carboxyl groups are formed in both the oxidation and hydrolysis reactions, and the formation of carbonyl groups in the cellulose chains is suggested as a responsible factor for the degradation of cellulose with concomitant color-change (Lojewska et al., 2007; Yatagai & Zeronian, 1994). This formation of carboxyl groups during the degradation can also be related to the decrease in pH (see Tables 3 and 4). Additionally, colored low-molecular furan-type compounds can be formed in the thermal degradation of carbohydrates such as glucose, and it is therefore also a possibility that these compounds can cause a color-change in cellulose samples incubated at higher temperatures (Nie et al., 2013; Ramchander & Feather, 1975). This is further discussed below.

The color of the films prepared from nanocellulose dispersions was assessed based on digitally scanned images. Examples of scanned films of TEMPO-CNF without additives and with Na-formate are shown in Fig. 3A. The images indicate that the color-change at increasing temperatures was consequently largest for the nanocelluloses without Na-formate. The highest charged nanocelluloses (Carboxy-CNF and TEMPO-CNF, see Table 2) had the highest color-change, ranging from roughly 45 to 65% (Fig. 3B). The Mech-CNF and CNC showed less color-change. The color-change is an indication of decomposition of the nanocelluloses, and this was confirmed by SEM analysis. The assessment revealed that the Mech-CNF and CNC kept the typical fibrillar/crystal structure even after 150 °C (Fig. S.2 in Supplementary material), compared to the Carboxy- and in particular the TEMPO-CNF where clear signs of degradation was observed (Fig. S.2 in Supplementary material).

Table 5
Estimation of HMF/furfural concentration in the different nanocellulose dispersions after heat aging at 140 °C for 3 days.

Sample code	HMF/furfural after heat aging at 140 °C for 3 days (mg/l)	
	Without additive	Sodium formate
Mech-CNF	32	12
CNC	1	4
TEMPO-CNF	336	205
Carboxy-CNF	157	66
Xanthan	414	230
Guar gum	742	232

3.5. Determination of degradation products

The samples used in this study are carbohydrate polymers with hexose and pentose monomers in various proportions. The hexoses can, when exposed to heat and acid, undergo hydrolysis and degradation into hydroxymethylfurfural (HMF), while the pentoses form furfural (Dunlop, 1948). The concentration of HMF/furfural was determined with UV–vis spectroscopy of the nanocellulose dispersions (Table 5). Furfural and HMF have similar absorbance spectra, and cannot be identified and/or separated from each other. Based on the quantification of the HMF/furfural concentration, the decomposition sequence was estimated as follows: Guar gum > xanthan > TEMPO-CNF > Carboxy-CNF > Mech-CNF > CNC. Interestingly, the nanocelluloses are less susceptible to degradation, compared to the conventional rheology modifiers xanthan and guar gum. This can be explained by the fact that the molecules in the bundle of the nanofibril/crystal are protected compared to single, dissolved molecules. A reduction in the concentration of HMF/furfural was observed for all the samples when sodium formate was used, except for the CNC sample in which the values were low both with and without additive. This is most probably due to the highly crystalline structure that makes CNC more resistant to degrade.

4. Conclusions

Thermostability of dispersions of the nanocelluloses Mech-CNF, TEMPO-CNF, Carboxy-CNF and CNC, have been studied by heat aging at temperatures ranging from 110 to 150 °C. Additives that either stabilize pH or act as radical scavengers have been used in order to shed light over the degradation mechanisms. The results indicate that ORD is the main mechanism as addition of the radical scavengers cesium formate or sodium formate reduced

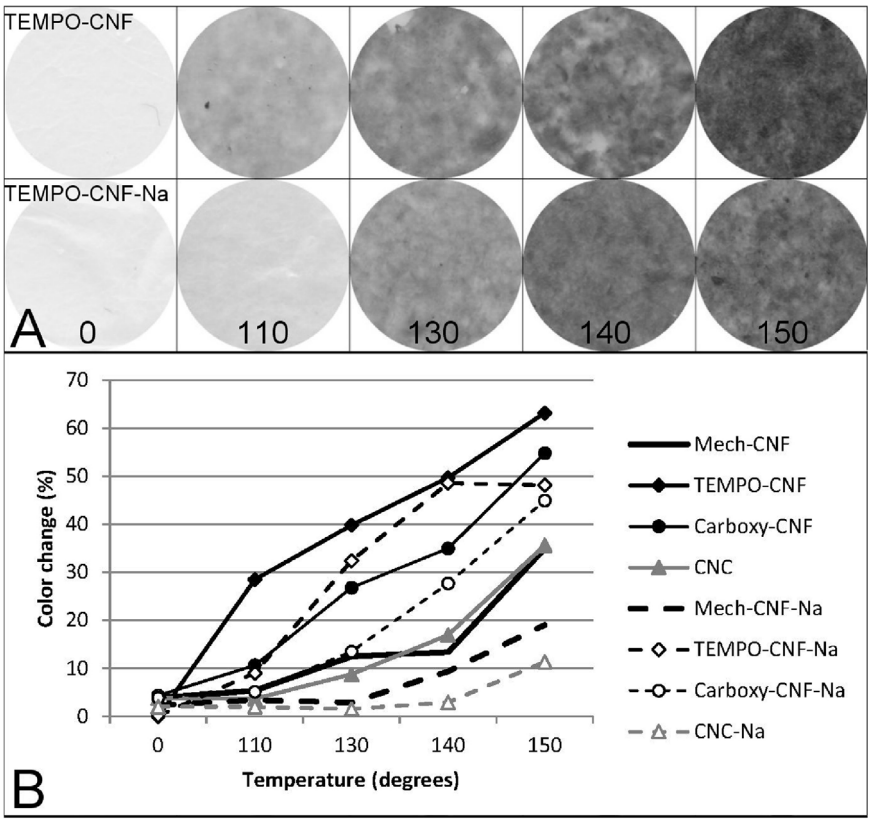

Fig. 3. (A) Local areas of scanned films, TEMPO samples. From left to right, films after 0, 110, 130, 140, 150 °C. (Upper row) TEMPO without additive. (Lower row) TEMPO and Na-formate. (B) Color-change as a function of temperature. The change in color was measured for the four different nanocellulose qualities both without additives and with Na-formate.

thermal degradation considerably. The analyzes show clearly that the nanocelluloses start to degrade already at 110 °C, which is at a much lower temperature compared to experiments described in literature performed in dry state. Comparison of the nanocelluloses showed that there are differences between the nanocellulose qualities tested; Mech-CNF and CNC were the most stable qualities, being stable after heat aging to 140 °C for three days when using formate as additive. All the nanocelluloses assessed in this study had better temperature stability than guar gum and xanthan, which indicates that nanocelluloses show promise as rheology modifiers for drilling fluids in oil wells.

Acknowledgements

This work has been carried out as a part of the WaterFlu project partly funded by the Research Council of Norway through the grant 217212 and the GreenEOR project funded by the Research Council of Norway through the grant 244615/E30 in the Petromaks2 programme. Elkem, Statoil and Treklyngen are all thanked for additional financial support, and Cabot are thanked for providing cesium formate. Anne Marie Reitan, Ingebjørg Leirset and Kristin Stensønes are thanked for their skilful technical assistance.

Appendix A. Supplementary data

Supplementary data associated with this article can be found, in the online version, at http://dx.doi.org/10.1016/j.carbpol.2016.09.077.

References

Abidin, A. Z., Puspasari, T., & Nugroho, W. A. (2012). Polymers for enhanced oil recovery technology. *Procedia Chemistry*, *4*, 11–16.
Bras, J., Viet, D., Bruzzese, C., & Dufresne, A. (2011). Correlation between stiffness of sheets prepared from cellulose whiskers and nanoparticles dimensions. *Carbohydrate Polymers*, *84*(1), 211–215.
Brinchi, L., Cotana, F., Fortunati, E., & Kenny, J. M. (2013). Production of nanocrystalline cellulose from lignocellulosic biomass: Technology and applications. *Carbohydrate Polymers*, *94*(1), 154–169.
Caenn, R., & Chillingar, G. V. (1996). Drilling fluids: State of the art. *Journal of Petroleum Science and Engineering*, *14*(3–4), 221–230.
Chang, H. L. (1978). Polymer flooding technology – Yesterday, today, and tomorrow. *Journal of Petroleum Technology*, 1113–1128.
Chen, L., Zhu, J. Y., Baez, C., Kitin, P., & Elder, T. (2016). Highly thermal-stable and functional cellulose nanocrystals and nanofibrils produced using fully recyclable organic acids. *Green Chemistry*, *18*(13), 3835–3843.
Chinga-Carrasco, G., Yu, Y. D., & Diserud, O. (2011). Quantitative electron microscopy of cellulose nanofibril structures from eucalyptus and pinus radiata kraft pulp fibers. *Microscopy and Microanalysis*, *17*(4), 563–571.
Chinga-Carrasco, G., Kuznetsova, N., Garaeva, M., Leirset, I., Galiullina, G., Kostochko, A., et al. (2012). Bleached and unbleached MFC nanobarriers: Properties and hydrophobisation with hexamethyldisilazane. *Journal of Nanoparticle Research*, *14*(12)
Dong, X. M., Revol, J. F., & Gray, D. G. (1998). Effect of microcrystallite preparation conditions on the formation of colloid crystals of cellulose. *Cellulose*, *5*(1), 19–32.
Downs, J. D. (1992). High-temperature stabilization of xanthan in drilling-fluids by the use of formate salts. *Physical Chemistry of Colloids and Interfaces in Oil Production*, *50*, 197–202.
Dunlop, A. P. (1948). Furfural formation and behavior. *Industrial and Engineering Chemistry*, *40*(2), 204–209.
Force (2011). Assessment of Environmental Impact from EOR Chemicals for the Norwegan Continental Shelf.
Fukuzumi, H., Saito, T., Okita, Y., & Isogai, A. (2010). Thermal stabilization of TEMPO-oxidized cellulose. *Polymer Degradation and Stability*, *95*(9), 1502–1508.
Habibi, Y., Lucia, L. A., & Rojas, O. J. (2010). Cellulose nanocrystals: Chemistry, self-assembly, and applications. *Chemical Reviews*, *110*(6), 3479–3500.
Henriksson, M., Henriksson, G., Berglund, L. A., & Lindstrom, T. (2007). An environmentally friendly method for enzyme-assisted preparation of

microfibrillated cellulose (MFC) nanofibers. *European Polymer Journal*, *43*(8), 3434–3441.
Herrick, F. W., Casebier, R. L., Hamilton, J. K., & Sandberg, K. R. (1983). Microfibrillated cellulose: Morphology and accessibility. *Journal of Applied Polymer Science Applied Polymer Symposium*, *37*, 797–813.
Howard, S., Kaminski, L., & Downs, J. (2015). Xanthan stability in formate brines – formulating non-damaging fluids for high temperature applications. *Society of Petroleum Engineers, SPE-174228-MS*, 1–18.
Iotti, M., Gregersen, Ø. W., Moe, S., & Lenes, M. (2011). Rheological studies of microfibrillar cellulose water dispersions. *Journal of Polymers and the Environment*, *19*(1), 137–145.
Johnson, R. K., Zink-Sharp, A., Renneckar, S. H., & Glasser, W. G. (2009). A new bio-based nanocomposite: Fibrillated TEMPO-oxidized celluloses in hydroxypropylcellulose matrix. *Cellulose*, *16*(2), 227–238.
Julien, S., Chornet, E., & Overend, R. P. (1993). Influence of acid pretreatment (H2so4,Hcl,Hno3) on reaction selectivity in the vacuum pyrolysis of cellulose. *Journal of Analytical and Applied Pyrolysis*, *27*(1), 25–43.
Klemm, D., Kramer, F., Moritz, S., Lindström, T., Ankerfors, M., Gray, D., et al. (2011). Nanocelluloses: A new family of nature-Based materials. *Angewandte Chemie-International Edition*, *50*(24), 5438–5466.
Kleppe, P. J. (1970). Kraft pulping. *Tappi*, *53*(1), 35-&.
Lin, N., Huang, J., & Dufresne, A. (2012). Preparation, properties and applications of polysaccharide nanocrystals in advanced functional nanomaterials: A review. *Nanoscale*, *4*(11), 3274–3294.
Lojewska, J., Missori, M., Lubanska, A., Grimaldi, P., Zieba, K., Proniewicz, L. M., et al. (2007). Carbonyl groups development on degraded cellulose. Correlation between spectroscopic and chemical results. *Applied Physics A—Materials Science & Processing*, *89*(4), 883–887.
Matsuo, M., Umemura, K., & Kawai, S. (2012). Kinetic analysis of color changes in cellulose during heat treatment. *Journal of Wood Science*, *58*(2), 113–119.
McClements, D. J. (2004). Emulsion rheology. In *Food emulsions – Principles, practices and techniques*. CRC Press., 632 p.
Nie, S. P., Huang, J. G., Hu, J. L., Zhang, Y. N., Wang, S. A., Li, C., et al. (2013). Effect of pH, temperature and heating time on the formation of furan from typical carbohydrates and ascorbic acid. *Journal of Food Agriculture & Environment*, *11*(1), 121–125.
Pääkkö, M., Ankerfors, M., Kosonen, H., Nykänen, A., Ahola, S., Österberg, M., et al. (2007). Enzymatic hydrolysis combined with mechanical shearing and high-pressure homogenization for nanoscale cellulose fibrils and strong gels. *Biomacromolecules*, *8*(6), 1934–1941.
Rånby, B. G. (1951). The colloidal properties of cellulose micelles. *Discussions of the Faraday Society*, *11*, 158–164.
Ramchander, S., & Feather, M. S. (1975). Studies on mechanism of color formation in glucose syrups. *Cereal Chemistry*, *52*(2), 166–173.
Roman, M., & Winter, W. T. (2004). Effect of sulfate groups from sulfuric acid hydrolysis on the thermal degradation behavior of bacterial cellulose. *Biomacromolecules*, *5*(5), 1671–1677.
Rydholm, S. A. (1955). *Pulping processes*. Interscience Publisher.
Saito, T., & Isogai, A. (2004). TEMPO-mediated oxidation of native cellulose. The effect of oxidation conditions on chemical and crystal structures of the water-insoluble fractions. *Biomacromolecules*, *5*(5), 1983–1989.
Saito, T., Nishiyama, Y., Putaux, J. L., Vignon, M., & Isogai, A. (2006). Homogeneous suspensions of individualized microfibrils from TEMPO-catalyzed oxidation of native cellulose. *Biomacromolecules*, *7*(6), 1687–1691.
Sihtola, H., Kyrklund, B., Laamanen, L., & Palenius, I. (1963). Comparison and conversion of viscosity and DP-values determined by different methods. *Papper Och Trä – Specialnummer, 4a*, 225–232.
Thomas, S. (2008). Enhanced oil recovery – an overview. *Oil & Gas Science and Technology-Revue D Ifp Energies Nouvelles*, *63*(1), 9–19.
Turbak, A. F., Snyder, F. W., Sandberg, K. R. (1982). Food products containing microfibrillated cellulose. (Vol. US Patent no. 4341807).
Turbak, A. F., Snyder, F. W., & Sandberg, K. R. (1983). Microfibrillated cellulose, a new cellulose product: Properties, uses, and commercial potential. *Journal of Applied Polymer Science*, *37*, 815–827.
Turbak, A. F., Snyder, F. W., & Sandberg, K. R. (1985). Suspensions containing microfibrillated cellulose. (Vol. US Patent no. 4500546).
Wågberg, L., Decher, G., Norgren, M., Lindström, T., Ankerfors, M., & Axnäs, K. (2008). The build-up of polyelectrolyte multilayers of microfibrillated cellulose and cationic polyelectrolytes. *Langmuir*, *24*(3), 784–795.
Wellington, S. L. (1983). Bio-Polymer solution viscosity stabilization – Polymer degradation and antioxidant use. *Society of Petroleum Engineers Journal*, *23*(6), 901–912.
Yatagai, M., & Zeronian, S. H. (1994). Effect of ultraviolet-light and heat on the properties of cotton. *Cellulose*, *1*(3), 205–214.
Zervos, S., & Moropoulou, A. (2005). Cotton cellulose ageing in sealed vessels. Kinetic model of autocatalytic depolymerization. *Cellulose*, *12*(5), 485–496.
Zhu, D. W., Wei, L. M., Wang, B. Q., & Feng, Y. J. (2014). Aqueous hybrids of silica nanoparticles and hydrophobically associating hydrolyzed polyacrylamide used for EOR in high-temperature and high-salinity reservoirs. *Energies*, *7*(6), 3858–3871.